Vocal fold contact pressure in a three-dimensional body-cover phonation model

Zhaoyan Zhang[a)]

Department of Head and Neck Surgery, University of California, Los Angeles, 31-24 Rehabilitation Center, 1000 Veteran Avenue, Los Angeles, California 90095-1794, USA

The goal of this study is to identify vocal fold geometric and mechanical conditions that are likely to produce large contact pressure and thus high risk of vocal fold injury. Using a three-dimensional computational model of phonation, parametric simulations are performed with co-variations in vocal fold geometry and stiffness, with and without a vocal tract. For each simulation, the peak contact pressure is calculated. The results show that the subglottal pressure and the transverse stiffness of the vocal folds in the coronal plane have the largest and most consistent effect on the peak contact pressure, indicating the importance of maintaining a balance between the subglottal pressure and transverse stiffness to avoiding vocal fold injury. The presence of a vocal tract generally increases the peak contact pressure, particularly for an open-mouth vocal tract configuration. While a low degree of vocal fold approximation significantly reduces vocal fold contact pressure, for conditions of moderate and tight vocal fold approximation changes in vocal fold approximation may increase or decrease the peak contact pressure. The effects of the medial surface thickness and vocal fold stiffness along the anterior−posterior direction are similarly inconsistent and vary depending on other control parameters and the vocal tract configuration. © 2019 Acoustical Society of America. https://doi.org/10.1121/1.5116138

Pages: 256–265

I. INTRODUCTION

Human voice production often involves repeated collision between the two vocal folds. The resulting contact pressure (also referred to as impact stress) between the two folds has generally been considered an important contributing factor toward vocal fold injury and the development of nodules, polyps, and cysts (Jiang and Titze, 1994; Titze, 1994). The goal of this study is to understand the biomechanics of vocal fold contact pressure and its dependence on the geometric and mechanical properties of the vocal folds. Specifically, we want to identify vocal fold geometric and mechanical parameters that have a global effect on vocal fold contact pressure across a large range of voice conditions so that they can be manipulated to consistently reduce contact pressure and thus risk of vocal fold injury. Such knowledge, together with an understanding of laryngeal muscular control of vocal fold posturing, would allow clinicians to better identify abusive vocal behaviors and recommend useful voice therapy strategies (Hillman *et al.*, 1989; Zhang, 2019). Such understanding may also benefit voice training by guiding singers to achieve their vocal goals while avoiding excessively large contact pressures (Titze, 2006).

There have been many previous studies to directly measure vocal fold contact pressure in human subjects (Reed *et al.*, 1990; Hess *et al.*, 1998; Verdolini *et al.*, 1999; Gunter *et al.*, 2005), excised animal and human larynges (Jiang and Titze, 1994), and physical models (Spencer *et al.*, 2008; Chen and Mongeau, 2011). In particular, Jiang and Titze (1994) conducted a comprehensive study of how changes in

vocal fold conditions affect the peak contact pressure. They showed that the peak contact pressure increased with increasing subglottal pressure or increasing vocal fold adduction. With increasing vocal fold elongation, the peak contact pressure first increased then decreased. Thus, their findings suggested large contact pressure at conditions of loud voice, hyperadduction, and high pitches. They also showed that peak contact pressure occurred at the midpoint of the membranous vocal folds, at which vocal nodules are often observed. One limitation of these experimental studies is that vocal fold geometry and stiffness were not simultaneously measured or controlled, and thus it is not possible to relate the contact pressure to the underlying geometric and mechanical conditions of the vocal folds. The limited spatial resolution of the pressure sensors used also prevented mapping out the contact pressure distribution in the glottis (Jiang and Titze, 1994). In particular, the location of peak contact pressure may vary significantly with vocal fold conditions and thus may not be captured by the sensors.

Computational models allow parametric variation of the geometry and mechanical conditions of the vocal folds and observing their effect on the contact pressure. Compared with lumped element models (e.g., Story and Titze, 1995), phonation models based on continuum mechanics allow examination of the contact pressure at a much finer resolution (Jiang *et al.*, 1998; Gunter, 2003, 2004; Tao *et al.*, 2006; Tao and Jiang, 2007; Bhattacharya and Siegmund, 2014, 2015; Granados *et al.*, 2017). Computational models also allow investigation of the mechanical stress within the vocal folds that is otherwise difficult to measure in experiments. Gunter (2003) showed that vocal fold contact pressure was directly correlated with the compressive stress, transverse shear stresses, and Von Mises stress, but not the longitudinal

a)Electronic mail: zyzhang@ucla.edu

0001-4966/2019/146(1)/256/10/$30.00

shear stress. Tao and Jiang (2007) further showed that the normal stress within the vocal fold was significantly lower than that on the surface. Consistent with experiments, these computational studies generally reported that the contact pressure decreases with decreasing subglottal pressure and that peak contact pressure occurs at mid-membranous locations. However, probably due to the high computational costs, there have been so far no systematic, parametric investigations of the dependence of contact pressure on vocal fold geometry and mechanical properties.

In the present study, parametric simulations are conducted in a three-dimensional body-cover phonation model (Zhang, 2017, 2018) to investigate the influence of vocal fold geometry and mechanical properties on the contact pressure between the two vocal folds. The advantage of such a computational approach is that the model control parameters (vocal fold geometry, mechanical properties, and vocal tract configuration) are varied one at a time so that the effect of individual control parameters on voice production can be isolated for investigation, which is almost impossible in animal or human models. Specifically, we parametrically vary the subglottal pressure, vocal fold approximation, medial surface vertical thickness, and vocal fold stiffness both in the transverse plane and along the anterior−posterior (AP) direction, all of which have been shown to have large influences on vocal control. Physiologically, these model parameters can be actively controlled, although not necessarily independently of each other, by laryngeal and respiratory muscle activation. For example, the subglottal pressure is primarily controlled by respiratory muscle activities. Both the transverse and AP stiffnesses of the vocal folds increase with vocal fold elongation and decrease with vocal fold shortening (Hirano and Kakita, 1985; Zhang et al., 2017), which can be controlled by the actions of the thyroarytenoid and cricothyroid muscles. Contraction of the thyroarytenoid muscle is expected to stiffen the body layer, both along the AP direction and in the transverse plane (Yin and Zhang, 2013). Vocal fold approximation is controlled by adductory and abductory muscles (Vahabzadeh-Hagh et al., 2017). The medial surface vertical thickness can be reduced by activation of the cricothyroid muscles, and increased by inferior-medial bulging of the medial surface due to the activation of the thyroarytenoid muscles (Hirano, 1988; Vahabzadeh-Hagh et al., 2017). The simulations are performed for three vocal tract conditions (without a vocal tract, and with vocal tract shapes corresponding to the /ɑ/ and /i/ sounds), to further evaluate potential effects of source−tract interaction on the contact pressure. In the following, the computational model, simulation conditions, and data analysis are first described in Sec. II. The results are presented in Sec. III, followed by discussions in Sec. IV.

II. METHOD

A. Computational model and simulation conditions

The same three-dimensional vocal fold model as in Zhang (2015, 2016, 2017) is used in this study. The reader is referred to these previous studies for details of the model. A sketch of the vocal fold model is shown in Fig. 1. Left−right
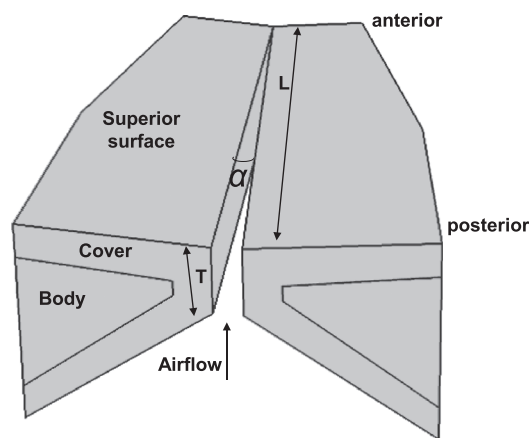

FIG. 1. The three-dimensional vocal fold model and key geometric control parameters, including the vocal fold length L along the AP direction, vertical thickness of the medial surface T, and the initial glottal angle α.

symmetry in vocal fold properties (geometry, material properties, and position) about the glottal midline is imposed so that only one vocal fold is modeled in this study. The vocal fold length along the AP direction is kept constant at 17 mm. The posterior cross-sectional geometry of the vocal fold has a medial-lateral depth of 6 and 1.5 mm in the body and cover layer, respectively, with a total depth of 7.5 mm. The cover layer thickness at the lateral boundary is set to be constant at 0.5 mm, based on measurements in Wu and Zhang (2016). The vocal fold cross-section tapers quadratically toward the anterior direction, with the total depth reduced to 3.75 mm at the anterior surface of the vocal folds, which results in a continuously reduced body-layer depth along the AP direction while the cover layer depth remains constant at 1.5 mm. The medial surfaces of the two vocal folds form an initial glottal angle α, changes in which control the resting glottal opening or degree of vocal fold approximation. The vocal fold model is fixed at the lateral surface and the two side surfaces at the anterior and posterior ends. The vocal fold model is developed in the commercial finite element software COMSOL. Depending on the specific vocal fold geometry, the model is discretized into about 120 000 total tetrahedral elements, and the medial surface is discretized with a resolution of about 0.2 mm along the AP direction and 0.01 − 0.05 mm along the vertical direction.

Each vocal fold layer is modeled as a transversely isotropic, nearly incompressible, linear material with a plane of isotropy perpendicular to the AP direction. The material control parameters for each vocal fold layer include the transverse Young's modulus E_t, the AP Young's modulus E_{ap}, the AP shear modulus G_{ap}, and density. The density of the vocal fold is assumed to be 1030 kg/m^3. The AP Poisson's ratio is assumed to be 0.495. As in previous studies (Zhang, 2017, 2018), to reduce the number of conditions to be investigated, the AP Young's modulus E_{ap} is assumed to be four times the AP shear modulus G_{ap}, and the transverse Young's moduli of the two layers are assumed to be identical in the present study. For both layers, a constant loss factor of 0.4 is used, similar to Zhang (2017, 2018). The glottal flow is modeled as a one-dimensional quasi-steady glottal flow model taking into consideration of viscous loss, as described in detail in

J. Acoust. Soc. Am. **146** (1), July 2019

Zhaoyan Zhang   257

Zhang (2015, 2017). Despite these simplifications, our previous studies using similar computational models have been able to reproduce experimental observations on voice production by unsteady glottal flow (Zhang *et al.*, 2002), phonation threshold pressure and frequency in a two-layer silicone vocal fold model (Farahani and Zhang, 2016), and vocal fold vibration patterns in different vibratory regimes and transitions between regimes (Zhang and Luu, 2012).

Vocal fold contact is modeled using the penalty method. Vocal fold contact occurs when portions of the vocal fold cross the glottal midline, in which case a penalty pressure along the medial-lateral direction into the vocal fold is applied to the contact surface of the vocal fold. A large enough penalty pressure will ensure small penetration depth of the vocal folds crossing the glottal midline, and the corresponding penalty pressure will approximate the true contact pressure. Although ideally larger penalty pressures provide more accurate solution of the contact pressure, too large of a penalty pressure often leads to numerical instabilities (Wriggers, 2006). In general, this penalty pressure is set to be proportional of the largest value of the system stiffness matrix. In this study, similar to Ishizaka and Flanagan (1972), the contact pressure p_c is related to the degree the vocal fold crosses the glottal midline Δy as follows (Zhang, 2015),

$$p_c = k_{c1}\omega_1^2 \Delta y (1 + k_{c2}\omega_1^2 \Delta y^2), \qquad (1)$$

where ω_1 is the first *in vacuo* angular eigenfrequency of the vocal fold, and $k_{c1} = 9$ and $k_{c2} = 6000$ are two contact coefficients, whose values are chosen to ensure small penetration depths while maintaining numerical stability. Note that k_{c1} and k_{c2} are not non-dimensional due to the way Eq. (1) is formulated, although they can be non-dimensionalized with a proper reformulation. For all the simulation conditions reported below, the mean penetration depth is about 0.002 mm, or about 1/750 of the cover layer depth (1.5 mm), indicating a reasonably good performance of the implemented penalty method.

The following model control parameters are varied (Table I), with the ranges of variation based on previous experimental and computational studies (Hollien and Curtis, 1960; Titze and Talkin, 1979; Hirano and Kakita, 1985; Alipour-Haghighi and Titze, 1991; Alipour *et al.*, 2000; Zhang *et al.*, 2017). Geometrically, the vertical thickness of the medial surface in the superior−inferior direction T is varied between 1–4.5 mm, as in our previous studies. The initial glottal angle α, which controls the degree of vocal fold approximation, is varied in three values equal to 0°, 1.6°, and 4° (a small set of simulations are also performed for

$\alpha = 8°$, as described below). Mechanically, the transverse stiffness of both layers E_t is varied in three values equal to 1, 2, and 4 kPa. The AP shear moduli in the cover and body layers, G_{apc} and G_{apb}, are each varied in five values equal to 1, 10, 20, 30, and 40 kPa, thus a total of 25 unique (G_{apc}, G_{apb}) conditions. The subglottal pressure is varied between 0 and 2.4 kPa, a total of 18 conditions that covers the range from soft voice to very loud voice. In total, this variation leads to 16200 parametric vocal fold conditions.

Three vocal tract conditions are considered in this study, without a vocal tract and with a vocal tract corresponding to either the /ɑ/ or /i/ sound. The first condition is a baseline condition, focusing on the effect of the laryngeal mechanisms alone. Comparison between this condition and the other two vocal tract conditions would identify the effects of vocal tract acoustic loading. The vocal tract is modeled as a one-dimensional waveguide (Story, 1995), and the cross-sectional area functions reported in Story *et al.* (1996) are used. No subglottal tract is included in the first condition without a vocal tract. For the other two conditions with a vocal tract, the model also includes an 11-cm long uniform subglottal tract.

In total, 16 200 conditions are investigated for each vocal tract conditions, with a total of 48 600 conditions. For each condition, a half-second of voice production is simulated using a fourth-order Runge-Kutta procedure (Zhang, 2015) at a sampling rate of 44 100 Hz, with the subglottal pressure linearly increased from zero to a target value in 30 time steps (about 0.68 ms) and then kept constant.

B. Data analysis

For each phonating condition, the peak contact pressure and its location on the medial surface are calculated. The peak contact area for each phonating condition is also calculated. These calculations are performed using the last 0.25 s of each simulation, by which time vocal fold vibration has either reached steady state or nearly steady state, or decayed into sufficiently small amplitude, to avoid the initial transients of the simulations. For each condition, the fundamental frequency F0 and sound pressure level (SPL) are also extracted, as described in Zhang (2016). The closed quotient of vocal fold vibration is calculated as the fraction of the cycle in which the glottal area function falls within the lower 10% between the minimum and maximum glottal area. Additionally, for each phonating condition, the produced voice is classified into one of three voice types (Titze, 1995): type 1 voice with a regular vocal fold vibration pattern, type 2 voice with a subharmonic vocal fold vibration, or type 3 with a chaotic vibration pattern, as described in Zhang (2018).

Our previous studies (Zhang, 2016, 2017, 2018) demonstrated interactions between physiologic control parameters in their effect on voice production. To focus on the effects of a specific control parameter that are consistent in a large range of vocal fold conditions, a histogram-based data analysis as described in Zhang (2017) is used in the present study to identify the global importance of specific control parameters to regulating the contact pressure. Specifically, for each of the six physiologic control parameters, changes in the peak contact

TABLE I. Ranges of model control parameters. For all conditions, the vocal fold density is 1030 kg/m³, the AP Poisson's ratio is 0.495, and $E_{ap} = 4\,G_{ap}$ is assumed. Note that a small set of simulations are also performed for $\alpha = 8°$, as described in the text.

Transverse Young's modulus	$E_t = [1, 2, 4]$ kPa
Cover AP shear modulus	$G_{apc} = [1, 10, 20, 30, 40]$ kPa
Body AP shear modulus	$G_{apb} = [1, 10, 20, 30, 40]$ kPa
Vertical thickness	$T = [1, 2, 3, 4.5]$ mm
Initial glottal angle	$\alpha = [0°, 1.6°, 4°]$
Subglottal pressure	$P_s = 50\text{–}2400$ Pa (18 conditions)

pressure due to incremental step increases (Table I) in the control parameter of interest while other control parameters remain constant are calculated, and a histogram of changes in peak contact pressure is generated for each of the six control parameters. A histogram with dominantly positive or negative values would indicate that changes in the corresponding control parameter would consistently increase or decrease the peak contact pressure across a large range of vocal conditions. To quantify this feature, for each histogram distribution X, a mean value M and a skewness factor S are calculated as below (Zhang, 2017),

$$M = \sum_{1}^{N} X/N,$$

$$S_1 = -\sum X^+ \Big/ \sum X^-,$$

$$S = \begin{cases} S_1, & S_1 >= 1 \\ -1/S_1, & S_1 < 1, \end{cases} \quad (2)$$

where N is the number of samples in the distribution X, and X^+ and X^- are subsets of X consisting of samples of positive and negative values, respectively. The mean value M quantifies the average expected change in the peak contact pressure due to a step increase in a specific control parameter. The absolute value of the skewness factor S, the ratio between the numbers of samples in X^+ and X^-, quantifies the likelihood that an increase in a control parameter consistently increases or decreases the peak contact pressure, whereas the sign of S indicates the direction of change (i.e., an increase or decrease in the peak contact pressure). As in Zhang (2017), in this study, a control parameter is considered to have a significant and consistent effect on the peak contact pressure if the absolute value of the corresponding S value is larger than 5 and the absolute M value is more dominant than that of other control parameters.

III. RESULTS

A. Comparison to previous experiments

Figure 2 shows a typical waveform of the intraglottal pressure at the middle point of the medial surface in the coronal plane. Also shown is the corresponding glottal area function. Similar to Jiang and Titze (1994), the intraglottal pressure consists of two contributions, the glottal air pressure when the vocal folds are not in contact at the specific location and the contact pressure when contact does occur. The peak contact pressure is about 1 kPa, compared to the subglottal pressure of 0.8 kPa. The waveform and magnitude of the intraglottal pressure is qualitatively similar to those reported in Jiang and Titze (1994; Figs. 7 and 9). There are also some notable differences. For example, in Fig. 2 the peak contact pressure occurs at an instant much closer to the instant of peak intraglottal air pressure than that in Fig. 7 of Jiang and Titze (1994). Note that in this study the relative phase of the contact pressure within the cycle and the relative magnitude between the peak contact pressure and peak glottal air pressure vary with the location on the medial surface as well as the vocal fold conditions, as further discussed below.

B. Contact pressure in the absence of a vocal tract

A stepwise multiple linear regression is performed on all phonating conditions to identify the overall dependence of the peak contact pressure on the six control parameters in the absence of a vocal tract. The standardized coefficients and R^2 values are shown in the second column of Table II (first value of each cell in the table). The linear regression shows a strong effect (with an absolute standardized coefficient greater than 0.1) of the subglottal pressure P_s, transverse stiffness E_t, vertical thickness T, and AP shear modulus in the cover layer G_{apc}. In comparison, although the effect of the initial glottal angle α and body-layer AP shear modulus G_{apb} is also statistically significant, the effect size (evaluated by the standardized coefficient) is much smaller.

While the linear regression captures the overall trend over the ranges of control parameters investigated, we are more interested in whether a change in a specific control parameter would consistently increase or decrease the peak contact pressure, regardless of the magnitude of the change or values of other control parameters. Figure 3 shows the histograms of changes in the peak contact pressure due to incremental step changes of each control parameter alone while other controls are kept constant. The corresponding M and S values are also shown. Consistent with the results from the
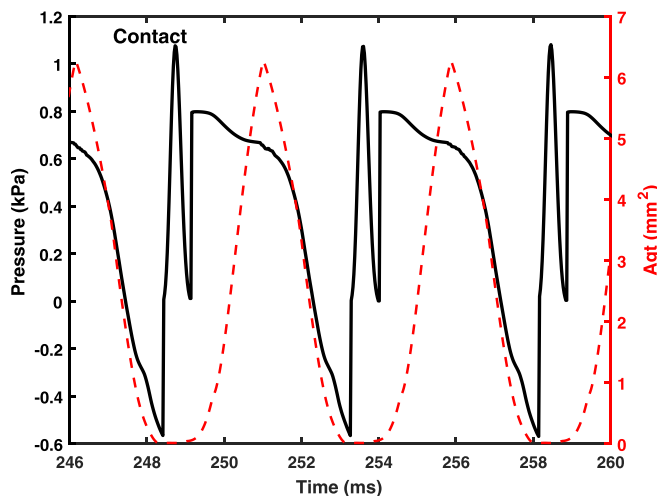

FIG. 2. (Color online) An example of the intraglottal pressure waveform (solid line) and glottal area function (dashed line). The subglottal pressure is 0.8 kPa.

TABLE II. Standardized coefficients and R^2 values of multiple linear regressions between the peak contact pressure (second column) and peak contact area (third column) and the six control parameters. The three values in each cell correspond to conditions without a vocal tract, with the /ɑ/ and /i/ vocal tract, respectively. * denotes parameters with $p > 0.005$ and thus statistically not significant. Standardized coefficients with absolute values greater than 0.1 are highlighted in bold.

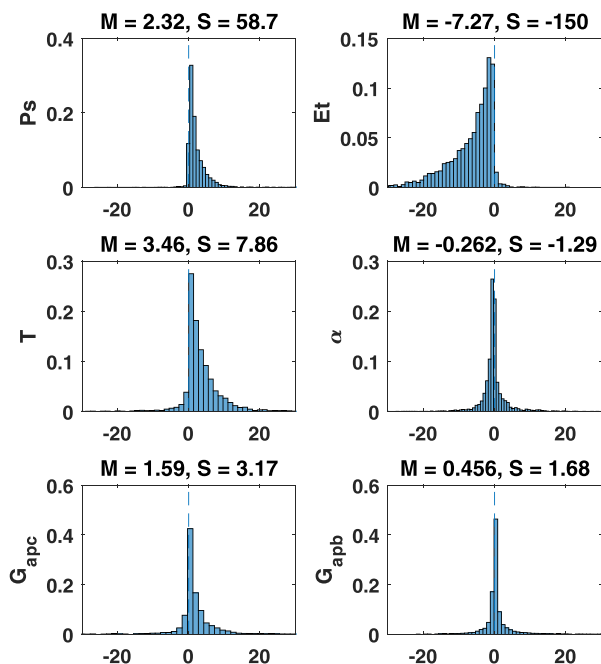|	Peak contact pressure	Peak contact area
P_s (kPa)	**0.730/0.728/0.731**	0.031/0.005*/0.061
E_t (kPa)	**−0.429/−0.362/−0.342**	−0.086/−0.054/−0.062
T (mm)	**0.284/0.131/0.075**	**0.832/0.812/0.812**
α (°)	−0.065/**0.100**/0.077	**−0.246/−0.219/−0.163**
G_{apc} (kPa)	**0.189**/0.069/0.003*	−0.042/−0.044/0.013*
G_{apb} (kPa)	0.034/**0.173/0.188**	−0.088/−0.037/0.057
R^2	0.676/0.620/0.609	0.747/0.683/0.673

FIG. 3. (Color online) Histograms of changes in the peak contact pressure due to incremental changes in the six control parameters (subglottal pressure P_s, stiffness E_t, medial surface vertical thickness T, initial glottal angle α, AP shear moduli in the cover and body layers G_{apc} and G_{apb}), for conditions without a vocal tract. Dashed lines indicate the origin or no changes in the peak contact pressure.

linear regression, the histogram analysis shows that the effects of the subglottal pressure P_s, transverse stiffness E_t, and vertical thickness T are quite consistent across the vocal fold conditions investigated, with the histograms consisting of values mostly on one side of the vertical axis and S values greater than 5. For the AP shear modulus in the cover layer G_{apc}, the histogram has a S value of 3.17, indicating that changes in the cover-layer AP stiffness increases the peak contact pressure in a majority of vocal fold conditions, but not as consistent as the subglottal pressure or transverse stiffness. In contrast, the effects of the initial glottal angle α and the body-layer AP shear modulus G_{apb} appear to be highly inconsistent and dependent on the values of other vocal fold parameters. Note that the M values quantify the amount of effect on the peak contact pressure due to a step change in the corresponding control parameter as specified in Table I. Comparison of the effect size between control parameters thus needs to consider both the relative M values and the corresponding step size in Table I.

The inconsistent effect of the initial glottal angle, or the degree of vocal fold approximation, is worth further elaboration. Figure 4 shows the effect of the initial glottal angle for two vocal fold conditions. The two conditions are identical except that the condition on the left has a higher cover-layer AP stiffness. For the range of initial glottal angle investigated (i.e., from 0° to 4°), the peak contact pressure decreases with increasing initial glottal angle in one condition (left column, top three rows in Fig. 4), but increases with the initial glottal angle in the other condition (right column, top three rows in Fig. 4). This appears to contradict previous experimental observation that the peak contact pressure decreases with increasing glottal gap (e.g., Jiang and Titze, 1994). We realize that the

range of initial glottal angle in this study covers those in normal phonation (Isshiki, 1989) but probably not those in a more open or breathy voice production. We have therefore conducted additional simulations for values of the initial glottal angle up to 8° for a small set of vocal fold conditions. As shown in Fig. 4, as the initial glottal angle further increases to 8°, the peak contact pressure decreases for both vocal fold conditions. In other words, the inconsistent effect of the initial glottal angle appears to exist only for conditions of tight and moderate vocal fold approximation (0°−4° as investigated in this study), and further reduction in vocal fold approximation eventually significantly reduces or completely eliminates the peak contact pressure, as observed in Jiang and Titze (1994).

C. Contact pressure in the presence of a vocal tract

To evaluate the effect of changes in vocal tract configurations, we compare the peak contact pressure for identical vocal fold conditions but different vocal tract configurations. Figure 5 shows the histograms of changes in the peak contact pressure due to changes in the vocal tract configuration (i.e., with vs without a vocal tract, /ɑ/ vs /i/ vocal tract). The first two histograms compare conditions with a vocal tract to those without a vocal tract. Both histograms consist primarily of positive values, indicating that the presence of a vocal tract increases the peak contact pressure. This is particularly the case for the /ɑ/ vocal tract, in which the peak contact pressure is almost doubled or tripled in some conditions compared to that without a vocal tract. The third histogram in Fig. 5, comparing the /ɑ/ vocal tract with the /i/ vocal tract, shows that the peak contact pressure is generally higher for the /ɑ/ vocal tract than that for the /i/ vocal tract.

Figures 6 and 7 show the histograms of changes in the peak contact pressure due to changes in the six control parameters for the /ɑ/ and /i/ vocal tract, respectively. Similar to those in Fig. 3 for conditions without a vocal tract, consistent effects (with large S values) of the subglottal pressure and transverse stiffness are observed in Figs. 6 and 7. In contrast, the effects of the vertical thickness and the cover-layer AP shear modulus are no longer as consistent across a large range of conditions in the presence of a vocal tract. On the other hand, the body-layer AP shear modulus, which does not exhibit a consistent effect in the absence of a vocal tract, now shows a more consistent and significant effect for both vocal tracts. The initial glottal angle also now shows a more consistent effect in the presence of a vocal tract. However, note again that such effect disappears when the initial glottal angle is further increased beyond 4°, as shown in Fig. 4. These observations are confirmed by the stepwise linear regression shown in Table II.

D. Contact area and location of peak contact

In general, the peak contact area increases with increasing vertical thickness or decreasing initial glottal angle, as shown by the multiple linear regression in the third column of Table II. The regression also shows a weak effect of the transverse stiffness and AP shear moduli in the body and cover layers, with the peak contact area decreasing with an increase in either modulus (except for conditions with the /i/
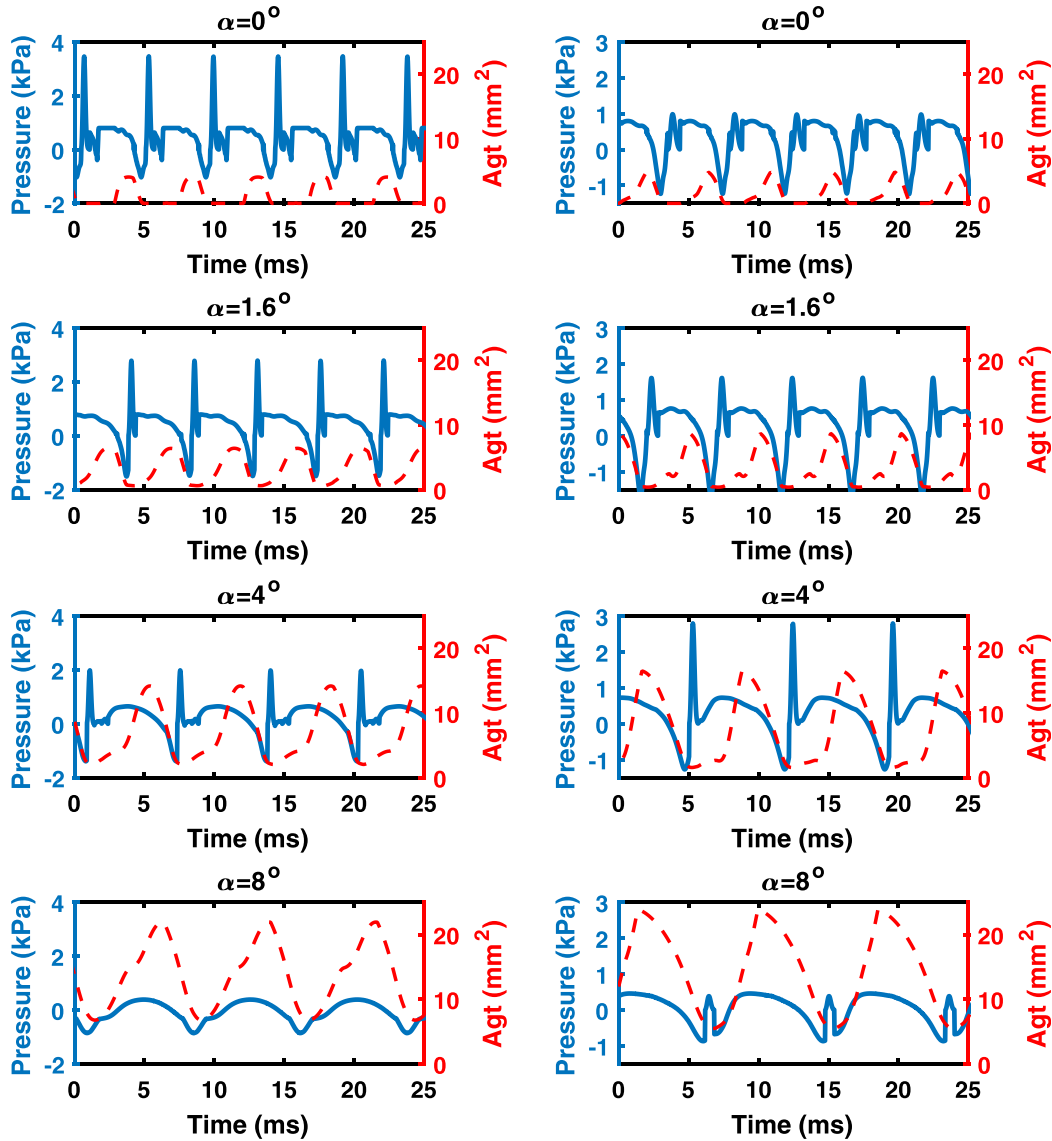
FIG. 4. (Color online) Effect of the initial glottal angle on the intraglottal pressure (solid lines) and glottal area function (dashed lines) for two typical vocal fold conditions. Left: the peak contact pressure decreases monotonically with increasing initial glottal angle, whereas on the right column the peak contact pressure reaches maximum at $\alpha = 4°$ before it decreases with further increase in the initial glottal angle. The two vocal fold condition are identical ($T = 3$ mm, $E_t = 4$ kPa, $G_{apb} = 10$ kPa, $P_s = 0.8$ kPa) except the left condition has a higher cover-layer AP stiffness ($G_{apc} = 30$ kPa) than the right ($G_{apc} = 10$ kPa).

vocal tract). Table II also shows a slight effect of the subglottal pressure, with the peak contact area increasing slightly with increasing subglottal pressure. However, a much larger effect of the subglottal pressure is observed when regression is performed over conditions with the subglottal pressure lower than 1 kPa (typical of normal speech), in which increasing subglottal pressure significantly increases the peak contact pressure. This large effect of the subglottal pressure in the lower range is probably because an increase in the subglottal pressure would significantly improve vocal fold contact at low subglottal pressure but this effect becomes less significant at increasingly higher subglottal pressures (Zhang, 2016).

Figure 8 shows the histograms of the location of peak contact pressure along the AP direction for all three vocal tract configurations. Note that the anterior and posterior ends of the vocal fold are at 0 and 17 mm in the figure, respectively. In general, the peak contact pressure is most likely to occur at the middle region along the AP direction, as

indicated by a cluster of data points around 7–10 mm in the figure, which is consistent with the findings in Jiang and Titze (1994). There are a considerable number of vocal fold conditions in which the peak contact pressure occurs at regions close to the anterior and posterior ends (around 2 mm and 14 − 15 mm). This is partially because that due to close proximity to the glottal centerline (see Fig. 1) and the fixed boundary condition at the anterior end, the most anterior locations (and the most posterior locations for conditions with $\alpha = 0°$) of the vocal folds almost always vibrate with contact. Similar tendency of contact at anterior locations has been reported in Lohscheller et al. (2013), which showed that the open quotient decreased significantly toward the anterior end of the vocal folds in humans. Vocal fold contact at anterior and posterior locations is also facilitated by weak excitation of AP modes (i.e., different portions of the vocal folds along the AP direction vibrate at different phases) with local displacement maxima at these locations, which in this
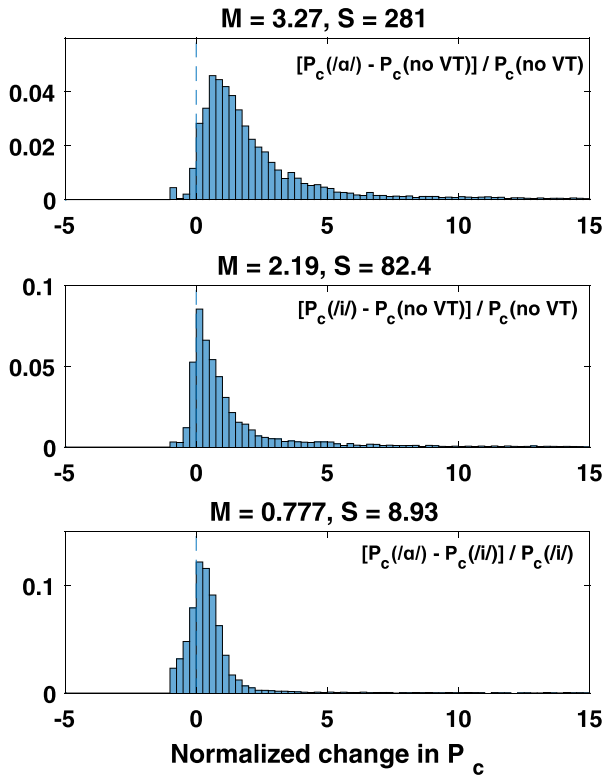
J. Acoust. Soc. Am. **146** (1), July 2019

Zhaoyan Zhang   261

FIG. 5. (Color online) Histograms of differences in the peak contact pressure between conditions with the /ɑ/ vocal tract and without a vocal tract (top), between conditions with the /i/ vocal tract and without a vocal tract (middle), and between conditions with the /ɑ/ and /i/ vocal tract. Dashed lines indicate the origin (i.e., no changes between vocal tract conditions).

study is often observed in vocal folds with isotropic or nearly isotropic stiffness conditions, consistently with our previous experimental [Fig. 3(b) in Mendelsohn and Zhang, 2011] and numerical studies (Fig. 5 in Zhang, 2014). Although the contact pressure at these anterior and posterior locations is in general small due to the relatively small vibration amplitude, peak contact pressure may occur at these locations in the absence of strong mid-membranous contact (e.g., vocal folds with a small vertical thickness or a large initial glottal angle). As the initial glottal angle increases, there is also a tendency of the posterior location of peak contact pressure to gradually move anteriorly.

E. Correlations with F0, SPL, closed quotient, and voice type

Because measurement of vocal fold geometry and stiffness is often difficult in human subjects, it is of interest to examine the correlation between the peak contact pressure and the fundamental frequency F0, vocal intensity SPL, closed quotient of vocal fold vibration, and voice type, which are relatively easier to measure. Table III shows the standardized coefficients and R^2 values of simple linear regression between the peak contact pressure and the three individual output measures of voice production. Vocal intensity SPL has the highest correlation with the peak contact pressure, followed by the CQ, with the F0 showing the smallest correlation. While the R^2 values are considerable for SPL, they are much smaller for CQ and F0, indicating a small effect size for both F0 and CQ. It should be
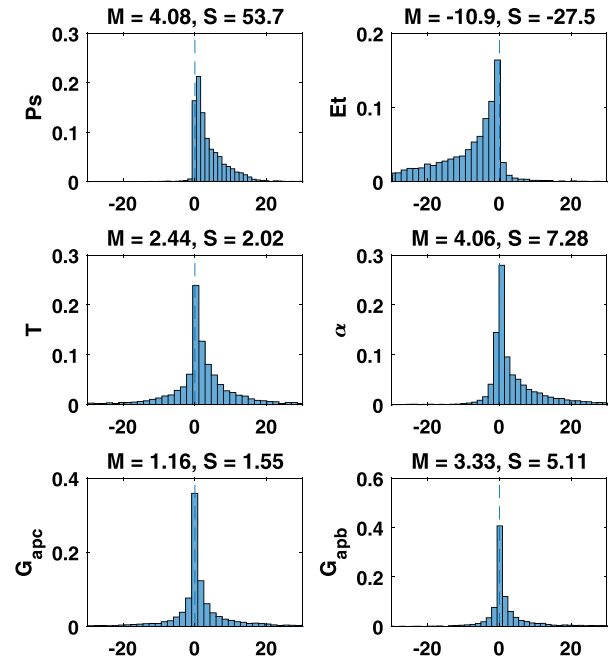

FIG. 6. (Color online) Histograms of changes in the peak contact pressure due to incremental changes in each of the six control parameters alone, for conditions with the /ɑ/ vocal tract. Dashed lines indicate the origin or no changes in the peak contact pressure.

noted that the model control parameters in this study are varied independent of each other, whereas they often co-vary in humans. Such co-variations among the model control parameters may lead to different correlations in humans from those reported here.

Analysis of variance shows statistically significant effects ($p < 0.005$) of the voice type (types 1, 2, and 3) on
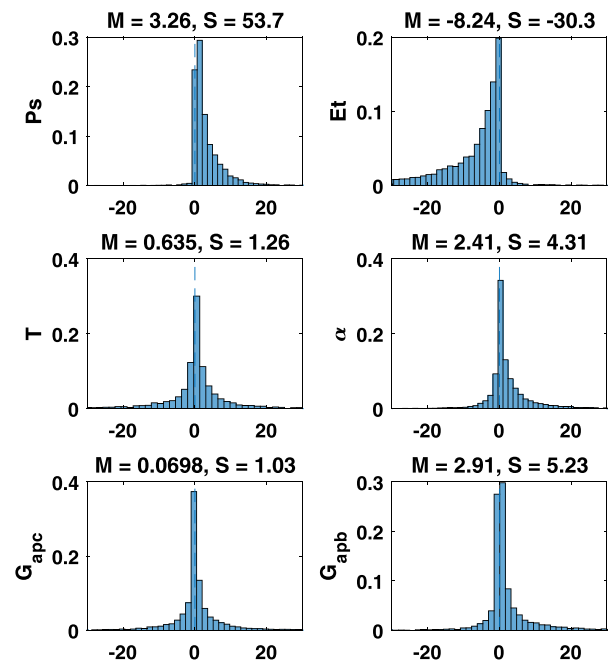

FIG. 7. (Color online) Histograms of changes in the peak contact pressure due to incremental changes in each of the six control parameters alone, for conditions with the /i/ vocal tract. Dashed lines indicate the origin or no changes in the peak contact pressure.
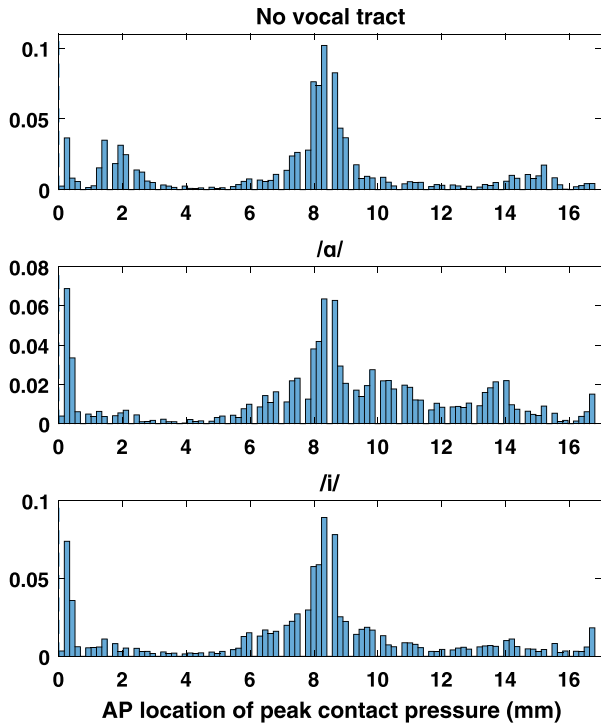
FIG. 8. (Color online) Histograms of the AP location of peak contact pressure for conditions without a vocal tract (top), with the /ɑ/ vocal tract (middle), and with the /i/ vocal tract (bottom). The anterior and posterior ends of the vocal fold are at 0 and 17 mm, respectively.

the peak contact pressure [$F(2,11523) = 546.3$ for conditions without a vocal tract, $F(2, 11523) = 190.2$ for the /ɑ/ vocal tract, and $F(2, 11583) = 733.7$ for conditions with the /i/ vocal tract], although the large sample size (i.e., the number of conditions) may have at least partially contributed to the small p values. Indeed, the R^2 values are generally small: 0.112, 0.032, 0.112 for conditions without a vocal tract, with the /ɑ/ vocal tract, and the /i/ vocal tract, respectively. Multiple comparison shows that, for conditions without a vocal tract or with the /i/ vocal tract, the peak contact pressure is the highest for type 3, followed by type 2, and is the lowest for type 1 voices. For conditions with the /ɑ/ vocal tract, the peak contact pressure in types 2 and 3 voices is higher than in type 1, but there is no statistically significant difference between peak contact pressure in types 2 and 3.

F. Vocal fold conditions with a stiffer body layer

Although indentation testing showed that the thyroarytenoid muscle, which forms the body layer of the vocal fold, was softer than the cover layer when dissected from the

TABLE III. Standardized coefficients and R^2 values of simple linear regressions between the peak contact pressure and F0, SPL, and CQ, respectively. The three values in each cell correspond to conditions without a vocal tract, with the /ɑ/ and /i/ vocal tract, respectively. * denotes parameters with $p > 0.005$ and thus statistically not significant.

	Standardized Coefficient	R^2
F0 (Hz)	−0.018*/−0.111/−0.149	3.16e−4*/0.012/0.022
SPL (dB)	0.515/0.583/0.563	0.265/0.339/0.318
CQ	0.358/0.280/0.314	0.128/0.078/0.098

laryngeal framework (Chhetri *et al.*, 2011), the body layer is generally expected to be stiffer than the cover layer (Yin and Zhang, 2013). The analysis above is repeated to consider only vocal fold conditions in which the body layer AP stiffness is greater than or equal to that of the cover layer. The results are generally similar to those obtained when all vocal fold conditions are considered. Imposing the body layer to be stiffer than the cover layer does lead to an even smaller effect of the body-layer AP stiffness, which otherwise has a sizeable effect on the peak contact pressure in the presence of a vocal tract (Table II).

IV. DISCUSSION AND CONCLUSIONS

This study shows that the subglottal pressure and the transverse stiffness of the vocal fold have the most consistent and dominant effect on the peak contact pressure. In almost all conditions investigated, the peak contact pressure consistently decreases with decreasing subglottal pressure or increasing transverse stiffness. Our results also show a strong effect of the vocal tract, with the peak contact pressure generally much higher in the presence of a vocal tract, particularly for the /ɑ/ vocal tract with an open-mouth configuration. In contrast, the effects of the other four control parameters (body and cover AP stiffnesses, initial glottal angle, and vertical thickness) are less consistent and vary depending on the specific vocal fold and vocal tract conditions. Specifically, in the absence of a vocal tract, an increase in either the medial surface vertical thickness or the cover-layer AP stiffness often increases the peak contact pressure, although this trend becomes less consistent when a vocal tract is added. The body-layer AP stiffness has a more consistent and positive effect on the peak contact pressure in the presence of a vocal tract, which disappears for conditions with a body layer stiffer than the cover layer or for conditions without a vocal tract. While a low degree of vocal fold approximation significantly reduces vocal fold contact pressure, for conditions of moderate and tight vocal fold approximation an increase in the initial glottal angle may increase or decrease the peak contact pressure, depending on vocal fold stiffness and vocal tract conditions.

Our results also show that the peak contact pressure has a significant and positive correlation with vocal intensity, which is consistent with the positive relation between the peak contact pressure and the subglottal pressure. Statistically significant correlation is also observed between the peak contact pressure and the closed quotient and voice type, with the peak contact pressure increasing with increasing closed quotient and being higher in non-modal phonation (type 2 and 3 voices) than in modal phonation (type 1 voice). However, the effect sizes for both the closed quotient and voice type are small, with R^2 values less than 0.1. A negative correlation between the peak contact pressure and F0 is also observed in the presence of a vocal tract, but with an even smaller effect size.

These results are largely consistent with previous findings. For example, the large positive effect of the subglottal pressure on the peak contact pressure has been consistently reported in previous studies (Jiang and Titze, 1994; Tao *et al.*, 2006; Galindo *et al.*, 2017). The peak contact pressure often occurs at the middle region along the AP direction,

J. Acoust. Soc. Am. **146** (1), July 2019

Zhaoyan Zhang 263

consistent with Jiang and Titze (1994) and other numerical studies (Tao *et al.*, 2006; Tao and Jiang, 2007). As the initial glottal angle increases, the peak contact pressure eventually decreases and disappears, consistent with the observation in Jiang and Titze (1994) regarding the effect of adduction. The weak relation between the closed quotient and peak contact pressure is consistent with the observation in human subjects in Verdolini *et al.* (1999). It appears that an increase in the duration of the closed phase, which is primarily related to the vertical phase difference and vertical thickness of the medial surface (Zhang, 2016), does not necessarily indicate an increase in the depth of influence of vocal fold contact, which is directly related to the peak contact pressure.

Our study also reveals some trends that were not observed in previous experimental studies. For example, our study shows a strong interaction between the initial glottal angle and vocal fold AP stiffness, with the peak contact pressure in some stiffness conditions varying with the initial glottal angle in a non-monotonical manner for moderate and high degrees of vocal fold approximation. While this does not directly contradict previous findings, this trend needs to be verified in future experimental studies. Similarly, the occurrence of peak contact pressure at locations close to the anterior or posterior ends needs to be verified in future experiments.

Jiang and Titze (1994) reported that the peak contact pressure first increased then decreased with increasing vocal fold elongation. The effect of changes in vocal fold length is not investigated in this study. However, vocal fold elongation is often accompanied by an increase in both the transverse and AP vocal fold stiffness, vocal fold thinning, and possibly a slight decrease in vocal fold approximation (Hirano and Kakita, 1985). While increasing transverse stiffness and vocal fold thinning in the absence of a vocal tract would decrease peak contact pressure, increased AP stiffness in the cover layer would increase peak contact pressure. Depending on the degree of changes in vocal fold approximation, it may first increase then decrease the peak contact pressure (e.g., Fig. 4). Thus, the non-monotonic effect of vocal fold elongation observed in Jiang and Titze (1994) can be explained by the findings of this study. Nevertheless, a better understanding of the simultaneous geometric and mechanical changes in the vocal fold due to vocal fold elongation is required to better understand the observations in Jiang and Titze (1994).

The results of this study indicate that the most consistent strategy to avoid excessively high contact pressure, other than using a breathy voice, is to maintain a balance between the subglottal pressure and transverse stiffness to not overload the vocal folds during phonation. An extremely small transverse stiffness coupled with an extremely high subglottal pressure can lead to very high, vocal fold-damaging peak contact pressure. In other words, one should avoid producing a loud voice with a "relaxed" vocal fold condition. In humans, the lowest transverse stiffness often occurs in extremely relaxed conditions of the vocal folds with minimum elongation (Zhang *et al.*, 2017), as in soft voice or vocal fry, which is fortunately often produced with a low subglottal pressure. On the other hand, an increase in vocal intensity in humans often involves a simultaneous increase in both the subglottal pressure and laryngeal resistance (e.g., Isshiki, 1964) that is likely associated with increased transverse stiffness.

Our results show a generally lower peak contact pressure with the /i/ vocal tract compared to the /ɑ/ vocal tract, indicating the potential usefulness of a constricted vocal tract configuration in voice therapy. Titze (2006) showed that a semi-occluded vocal tract (e.g., with the use of a flow resistance tube attached to the mouth) reduces vibration amplitude and increases intraglottal pressure, both of which are expected to reduce vocal fold collision. He further hypothesized that "semi-occlusives allow the vocalist to build up high lung pressures without excessive damage to tissues due to large vibrational amplitudes." Our results appear to confirm this hypothesis. However, our results also show strong interaction between the vocal tract configuration and vocal fold properties (approximation, stiffness, and vertical thickness), as indicated by the inconsistent effect of the initial glottal angle, vocal fold AP stiffness, and vertical thickness. Future studies with more vocal tract configurations (e.g., those studied in Titze, 2006) are required to further elucidate potential effects of source tract interaction on vocal fold contact and contact pressure.

Vocal fold geometry and stiffness often co-vary in humans, partially because they are controlled by the same set of laryngeal muscles. Thus, translation of the findings of this study to human phonation has to take into consideration of these covariations. One example is vocal fold elongation as discussed earlier, which may increase or decrease the peak contact pressure, depending on the relative magnitude of the geometric and stiffness changes. Similarly, a strong correlation between F0 and the peak contact pressure may exist in humans, considering the covariations between the transverse and AP stiffnesses.

Another limitation of the present study is that the vocal fold is modeled as an elastic material, whereas in reality the vocal folds are viscoelastic and experience creep and stress relaxation, which is expected to affect the contact pressure. Furthermore, the vocal fold surface condition may affect adhesion and separation between the vocal folds, and is likely to play an important role in vocal fold contact and contact pressure (Bhattacharya and Siegmund, 2014, 2015; Tse *et al.*, 2015; Erath *et al.*, 2017), which needs to be considered in future studies.

ACKNOWLEDGMENTS

Alipour, F., Berry, D. A., and Titze, I. R. (**2000**). "A finite-element model of vocal-fold vibration," J. Acoust. Soc. Am. **108**, 3003–3012.

Alipour-Haghighi, F., and Titze, I. R. (**1991**). "Elastic models of vocal fold tissues," J. Acoust. Soc. Am. **90**, 1326−1331.

Bhattacharya, P., and Siegmund, T. (**2014**). "A computational study of systemic hydration in vocal fold collision," Comput. Methods Biomech. Biomed. Eng. **17**(16), 1835−1852.

Bhattacharya, P., and Siegmund, T. (**2015**). "The role of glottal surface adhesion on vocal folds biomechanics," Biomech. Model Mechanobiol. **14**, 283−295.

Chen, L., and Mongeau, L. (**2011**). "Verification of two minimally invasive methods for the estimation of the contact pressure in human vocal folds during phonation," J. Acoust. Soc. Am. **130**, 1618−1627.

Chhetri, D. K., Zhang, Z., and Neubauer, J. (**2011**). "Measurement of Young's modulus of vocal fold by indentation," J. Voice **25**, 1−7.

Erath, B. D., Zañartu, M., and Peterson, S. D. (**2017**). "Modeling viscous dissipation during vocal fold contact: The influence of tissue viscosity and thickness with implications for hydration," Biomech. Model Mechanobiol. **16**, 947−960.

Farahani, M., and Zhang, Z. (**2016**). "Experimental validation of a three-dimensional reduced-order continuum model of phonation," J. Acoust. Soc. Am. **140**, EL172−EL177.

Galindo, G., Peterson, S., Erath. B., Castro, C., Hillman, R., and Zanartu, M. (**2017**). "Modeling the pathophysiology of phontraumatic vocal hyperfunction with a triangular glottal model of the vocal folds," J. Speech Lang. Hear. Res. **60**, 2452−2471.

Granados, A., Misztal, M. K., Brunskog, J., Visseq, V., and Erleben, K. (**2017**). "A numerical strategy for finite element modeling of frictionless asymmetric vocal fold collision," Int. J. Numer. Meth. Biomed. Eng. **33**, e02793.

Gunter, H. E. (**2003**). "A mechanical model of vocal fold collision with high spatial and temporal resolution," J. Acoust. Soc. Am. **113**, 994−1000.

Gunter, H. E. (**2004**). "Modeling mechanical stresses as a factor in the etiology of benign vocal fold lesions," J. Biomech. **37**, 1119−1124.

Gunter, H. E., Howe, R., Zeitels, M., Kobler, J. B., and Hillman, R. (**2005**). "Measurement of vocal fold collision forces during phonation: Methods and preliminary data," J. Speech, Lang., Hear. Res. **48**, 567−576.

Hess, M. M., Verdolini, K., Bierhals, W., Mansmann, U., and Gross, M. (**1998**). "Endolaryngeal contact pressures," J. Voice **12**, 50−67.

Hillman, R., Holmberg, E., Perkell, J., Walsh, M., and Vaughan, C. (**1989**). "Objective assessment of vocal hyperfunction: An experimental framework and initial results," J. Speech Hear Res. **32**, 373−392.

Hirano, M. (**1988**). "Vocal mechanisms in singing: Laryngological and phoniatric aspects," J. Voice **2**, 51–69.

Hirano, M., and Kakita, Y. (**1985**). "Cover-body theory of vocal fold vibration," in *Speech Science: Recent Advances*, edited by R. G. Daniloff (College-Hill Press, San Diego), pp. 1−46.

Hollien, H., and Curtis, F. (**1960**). "A laminagraphic study of vocal pitch," J. Speech Hear. Res. **3**, 361−371.

Ishizaka, K., and Flanagan, J. L. (**1972**). "Synthesis of voiced sounds from a two-mass model of the vocal cords," Bell Syst. Tech. J. **51**, 1233−1267.

Isshiki, N. (**1964**). "Regulatory mechanism of voice intensity variation," J. Speech Hear. Res. **7**, 17−29.

Isshiki, N. (**1989**). *Phonosurgery: Theory and Practice* (Springer-Verlag, Tokyo), Chap. 3.

Jiang, J., Diaz, C., and Hanson, D. (**1998**). "Finite element modeling of vocal fold vibration in normal phonation and hyperfunctional dysphonia: Implications for the pathogenesis of vocal nodules," Ann. Otol. Rhinol. Laryngol. **107**, 603−610.

Jiang, J. J., and Titze, I. R. (**1994**). "Measurement of vocal fold intraglottal pressure and impact stress," J. Voice **8**(2), 132−144.

Lohscheller, J., Svec, J., and Döllinger, M. (**2013**). "Vocal fold vibration amplitude, open quotient, speed quotient and their variability along glottal length: Kymographic data from normal subjects," Logoped. Phoniatr. Vocol. **38**, 182−192.

Mendelsohn, A., and Zhang, Z. (**2011**). "Phonation threshold pressure and onset frequency in a two-layer physical model of the vocal folds," J. Acoust. Soc. Am. **130**, 2961−2968.

Reed, C., Doherty, T., and Shipp T. (**1990**). "Piezoelectric transducers for the direct measurement of medial forces in the glottis," J. Acoust. Soc. Am. **88**, S151−S151.

Spencer, M., Siegmund, T., and Mongeau, L. (**2008**). "Determination of superior surface strains and stresses, and vocal fold contact pressure in a synthetic larynx model using digital image correlation," J. Acoust. Soc. Am. **123**, 1089−1103.

Story, B. H. (**1995**). "Physiologically-based speech simulation using an enhanced wave-reflection model of the vocal tract," Ph.D. dissertation, University of Iowa, Chap. 2.

Story, B. H., and Titze, I. R. (**1995**). "Voice simulation with a body-cover model of the vocal folds," J. Acoust. Soc. Am. **97**, 1249−1260.

Story, B. H., Titze, I. R., and Hoffman, E. A. (**1996**). "Vocal tract area functions from magnetic resonance imaging," J. Acoust. Soc. Am. **100**, 537−554.

Tao, C., and Jiang, J. (**2007**). "Mechanical stress during phonation in a self-oscillating finite-element vocal fold model," J. Biomech. **40**, 2191−2198.

Tao, C., Jiang, J., and Zhang, Y. (**2006**). "Simulation of vocal fold impact pressures with a self-oscillating finite-element model," J. Acoust. Soc. Am. **119**(6), 3987−3994.

Titze, I. (**2006**). "Voice training and therapy with a semi-occluded vocal tract: Rationale and scientific underpinnings," J. Speech, Lang., Hear. Res. **49**, 448−459.

Titze, I., and Talkin, D. (**1979**). "A theoretical study of the effects of various laryngeal configurations on the acoustics of phonation," J. Acoust. Soc. Am. **66**, 60−74.

Titze, I. R. (**1994**). "Mechanical stress in phonation," J. Voice **8**, 99−105.

Titze, I. R. (**1995**). *Workshop on Acoustic Voice Analysis: Summary Statement*, National Center for Voice and Speech, Iowa City, IA, pp. 1−36.

Tse, J., Zhang, Z., and Long, J. L. (**2015**). "Effects of vocal fold epithelium removal on vibration in an excised human larynx model," J. Acoust. Soc. Am. **138**, EL60−EL64.

Vahabzadeh-Hagh, A., Zhang, Z., and Chhetri, D. (**2017**). "Quantitative evaluation of the *in vivo* vocal fold medial surface shape," J. Voice **31**, 513.e15−513.e23.

Verdolini, K., Hess, M. M., Titze, I. R., Bierhals, W., and Gross, M. (**1999**). "Investigation of vocal fold impact stress in human subjects," J. Voice **13**, 184−202.

Wriggers, P. (**2006**). *Computational Contact Mechanics* (Springer, New York), Chap. 6.

Wu, L., and Zhang, Z. (**2016**). "A parametric vocal fold model based on magnetic resonance imaging," J. Acoust. Soc. Am. **140**, EL159−EL165.

Yin, J., and Zhang, Z. (**2013**). "The influence of thyroarytenoid and cricothyroid muscle activation on vocal fold stiffness and eigenfrequencies," J. Acoust. Soc. Am. **133**, 2972−2983.

Zhang, Z. (**2014**). "The influence of material anisotropy on vibration at onset in a three-dimensional vocal fold model," J. Acoust. Soc. Am. **135**, 1480−1490.

Zhang, Z. (**2015**). "Regulation of glottal closure and airflow in a three-dimensional phonation model: Implications for vocal intensity control," J. Acoust. Soc. Am. **137**, 898−910.

Zhang, Z. (**2016**). "Cause-effect relationship between vocal fold physiology and voice production in a three-dimensional phonation model," J. Acoust. Soc. Am. **139**, 1493−1507.

Zhang, Z. (**2017**). "Effect of vocal fold stiffness on voice production in a three-dimensional body-cover phonation model," J. Acoust. Soc. Am. **142**, 2311−2321.

Zhang, Z. (**2018**). "Vocal instabilities in a three-dimensional body-cover phonation model," J. Acoust. Soc. Am. **144**(3), 1216−1230.

Zhang, Z. (**2019**). "Compensation strategies in voice production with glottal insufficiency," J. Voice **33**, 96−102.

Zhang, Z., and Luu, T. (**2012**). "Asymmetric vibration in a two-layer vocal fold model with left-right stiffness asymmetry: Experiment and simulation," J. Acoust. Soc. Am. **132**(3), 1626−1635.

Zhang, Z., Mongeau, L., and Frankel, S. H. (**2002**). "Experimental verification of the quasi-steady approximation for aerodynamic sound generation by pulsating jets in tubes," J. Acoust. Soc. Am. **112**(4), 1652−1663.

Zhang, Z., Samajder, H., and Long, J. (**2017**). "Biaxial mechanical properties of human vocal fold cover under vocal fold elongation," J. Acoust. Soc. Am. **142**, EL356−EL361.